

## Letters to the Editor

### To the Editor

One of the primary difficulties in quantitative backscattered electron (BSE) imaging has been to obtain calibrated, standardized images, which allow for comparison of results between studies. In the recent study by Roschger et al.,<sup>5</sup> the investigators modified previous calibration techniques in an effort to simplify the BSE analysis technique. Studies such as that performed by Roschger et al.<sup>5</sup> are important in the advancement of this technique.

We disagree, however, with their interpretation of the BSE histogram. Roschger et al.<sup>5</sup> suggest that the BSE gray-level histogram was an indication of the mineral density distribution; implying that the height of the histogram at any given location corresponded to the quantity of mineralized tissue of a given density. It has previously been demonstrated that the BSE signal is not a function of density, but rather a function of atomic number.<sup>1</sup> In bone, the BSE signal is most highly correlated with the weight fraction of mineral (weight mineral/weight bone tissue).<sup>2,6</sup> The description of the BSE signal as a density function is a misnomer. Furthermore, while it is undoubtedly true that mineral distributions affect the BSE histogram, as the authors have so nicely demonstrated, additional factors also influence histogram width. This can be clearly seen in comparative BSE histograms from human cortical bone and a pure (99.9999% pure) aluminum sample (full width at half maximum [FWHM] = 36 and 17 gray-levels, respectively; **Figure 1**). The large histogram width for aluminum suggests either that aluminum has a substantial "density distribution" or that as much as 50% of a bone's histogram width can be viewed as the result of the stochastic electron scattering process. Human cortical bone has a relatively broad histogram when compared with bones from other species,<sup>7</sup> thus the differences between bone and pure materials may be even smaller.

Roschger et al.<sup>5</sup> realized this limitation and suggested that histograms could be deconvoluted from histograms of pure compounds, but argued that the benefit would be "... sufficiently small to justify omission of this correction." We do not agree with this statement; BSE histograms are extremely variable using the method suggested by Roschger et al.<sup>5</sup> This can be demonstrated with a simple experiment. Three BSE images of a specimen containing pure C and Al were collected at probe currents

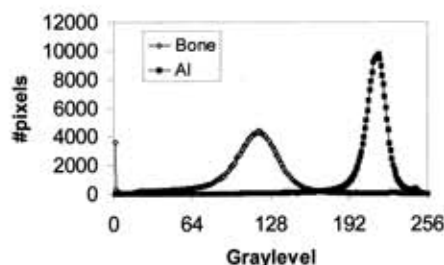


**Figure 1.** BSE histogram of aluminum and bone captured under identical operating conditions.

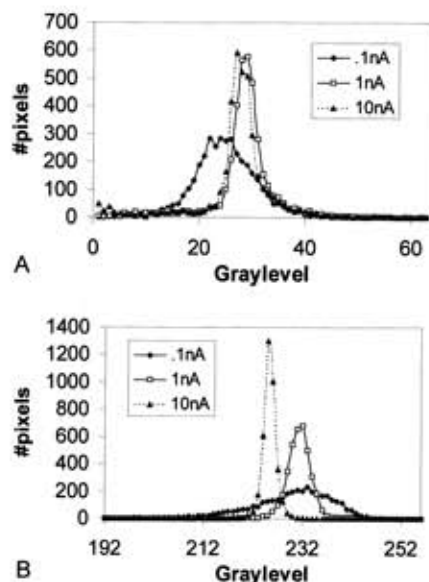


**Figure 2.** BSE histograms of carbon (A) and aluminum (B) analyzed in one operating session at three different probe currents.

of 0.1 nA, 1 nA, and 10 nA, respectively. Brightness and contrast settings were adjusted so that the mean C and Al gray levels remained calibrated in each image as previously described.<sup>5,7</sup> It is clear that the histogram width of both materials decreased dramatically with increasing probe current (**Figure 2**). For aluminum, FWHM was 16, 5, and 2, respectively. This represents an eightfold variation in the "mineral density distribution" for calibrated images. A similar effect can be achieved by varying the scan rate.

Given that BSE histogram widths are influenced by electron probe current, scan rates, and other factors, such as topography,<sup>4</sup> we do not believe that BSE histogram widths can be described in terms of their fractional calcium weight. Although we disagree with the authors' interpretation of the BSE histogram, it does not mean that the BSE histogram is not influenced by mineral variations. Within one study, relative comparisons of histogram widths are likely to be meaningful, and other investigators have adopted this approach.<sup>3,7</sup> The issue with the present study is the absolute quantitative values applied to the BSE histogram, which are likely to be erroneous due to the multitude of factors that affect BSE histograms. We suggest that investigators compare relative differences in histogram widths and refrain from the use of the term "mineral density."

### References

1. Bloebaum, R. D., Bachus, K. N., and Boyce, T. M. Backscattered electron imaging: The role in calcified tissue and implant analysis. *J Biomater Appl* 5:56-85; 1990.
2. Bloebaum, R. D., Skedros, J. G., Vajda, E. G., Bachus, K. N., and Constantz,

- B. R. Determining mineral content variations in bone using backscattered electron imaging. *Bone* 20:485–490; 1997.
- Boyd, A., Compston, J. E., Reeve, J., Bell, K. L., Noble, B. S., Jones, S. J., and Loveridge, N. Effect of estrogen suppression on the mineralization density of iliac crest biopsies in young women as assessed by backscattered electron imaging. *Bone* 22:241–250, 1998.
  - Howell, P. G. T. and Boyd, A. Monte Carlo simulations of electron scattering in bone. *Bone* 15:285–291; 1994.
  - Roschger, P., Fratzl, P., Eschberger, J., and Klaushofer, K. Validation of quantitative backscattered electron imaging for the measurement of mineral density distribution in human bone biopsies. *Bone* 23:319–326; 1998.
  - Roschger, P., Plenck, H., Jr., Klaushofer, K., and Eschberger, J. A new scanning electron microscopy approach to the quantification of bone mineral distribution: Backscattered electron image grey-levels correlated to calcium K $\alpha$ -line intensities. *Scann Microsc* 9:75–88; 1995.
  - Vajda, E. G., Skedros, J. G., and Bloebaum, R. D. Consistency in calibrated backscattered electron images of calcified tissues and mineral analyzed in multiple imaging sessions. *Scann Microsc* 9:741–755; 1995.

**E. G. Vajda**

*Division of Radiobiology  
University of Utah  
Salt Lake City, UT, USA*

**J. G. Skedros**

*Ogden Clinic  
Ogden, UT, USA*

## Response

Vajda and Skedros, in their Letter to the Editor, addressed two major points concerning our quantitated backscattered electron imaging (qBEI) method.<sup>1</sup> First, they criticized our use of the term “bone mineral density distribution” (BMDD) for our gray-level histograms, since we do not measure weight mineral/bone matrix volume (density), but rather degree of mineralization of the bone matrix in weight percent calcium.<sup>2,3</sup> We are aware of the fact that BMDD is not a precise term, but we introduced it for practical use in continuation of the term “bone mineral density” (BMD). Second, Vajda and Skedros doubt that a precise determination of the true distribution of mineral content in bone can be derived from the BE signal in the scanning electron microscope, as they show a number of gray-level distributions that vary greatly in width, when the experimental conditions of BEI are changed (see their Figures 1 and 2). We appreciate their pertinent remarks, which now give us the opportunity to explain some of our procedures more precisely.

We are convinced that—with proper precautions—it is possible to obtain quantitative data of mineral content in bone by using BEI. In what follows we compute the effects of counting statistics that lead to observed variations in the data and show how they can be minimized: Calling  $N$  the number of electrons hitting a given specimen position (area corresponding to a pixel in the BE image) and  $\nu$  the number of electrons scattered back into the detector, then the probability that  $\nu/N = x$  is given by the binominal distribution:

$$a(x, \rho) = \binom{N}{\nu} \rho^\nu (1 - \rho)^{N-\nu} \quad (1)$$

where  $\rho$  is the mean probability for backscattering within the specified pixel area.  $N$  is proportional to the incident electron current as well as to the counting time per pixel,  $t$ . When  $N$  is large enough, the standard approximation yields a gaussian for  $a(x, \rho)$ :

$$a(x, \rho) = \frac{1}{\sqrt{2\pi N\rho}} e^{-N[(x-\rho)^2/2\rho]} \quad (2)$$

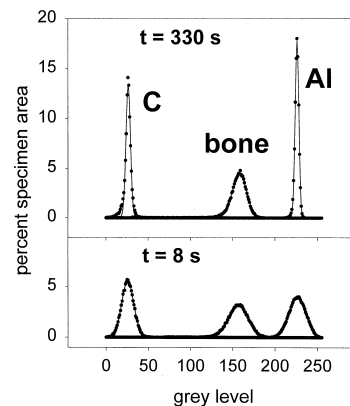


**Figure 1.** Backscattered electron gray-level histograms of carbon (C), aluminum (Al), and mineralized bone matrix (bone) obtained at two different counting times (scanning speeds). The other instrumental settings (C and Al calibration, probe current) were identical to those described in our study.<sup>1</sup> A dramatic effect of counting time on width of the C and Al gray-level distribution can be seen. By comparison, the effect on the gray-level distribution from bone was only moderate.

When a BE image is analyzed, every pixel will have its true electron backscattering probability and the true distribution,  $f(\rho)$ , is related to the measured gray-level distribution,  $g(x)$ , by:

$$g(x) = \int d\rho a(x, \rho) f(\rho) \quad (3)$$

If  $N$  was infinite (i.e., extremely large measuring time or electron current), then the distribution  $f(\rho)$  or  $g(x)$  would be the same. However, due to the effects of counting statistics,  $g(x)$  is usually broader than  $f(\rho)$ . **Figure 1** shows the gray-level distribution,  $f(x)$ , for two different counting times but otherwise identical instrumental settings. The measurement with shorter counting time gives a broader distribution because  $N$  is smaller in this case. In principle,  $f(\rho)$  can be obtained numerically from  $g(x)$  by inverting equation (3); however, to avoid this tedious deconvolution procedure (which may also introduce artifacts) we have chosen to operate under conditions in which distributions  $g(x)$  and  $f(\rho)$  are not too different. To be more precise, we have evaluated the effect of counting statistics on gaussian distributions of the type:

$$\frac{1}{\sqrt{2\pi b}} e^{-\frac{(\rho-\rho_o)^2}{2b^2}} \quad (4)$$

When  $f(\rho)$  has such a gaussian shape with width  $b = b_o$ , the integral (3) also yields, for  $g(x)$ , a gaussian, but with a width,  $b$ :

$$b^2 = b_o^2 + \rho_o/N \quad (5)$$

Again, when either the incident current or the measuring time become large,  $N$  becomes very large and  $b \approx b_o$ . On the other hand, the mean backscattering probability,  $\rho_o$ , is proportional to the atomic number ( $Z$ ), and hence depends linearly (at least in the  $Z$ -range considered) on the maximum position ( $M$ ) of the gray-level distribution. Introducing this into equation (5) the *measured width*,  $b$ , of a gray-level distribution can be described by:

$$b^2 = b_o^2 + K(M + M_o)/t \quad (6)$$

where  $b_o$  is the *true width* of the distribution.  $K$  and  $M_o$  are constants, depending on the instrumental setting, which can be determined experimentally as we see in what follows.

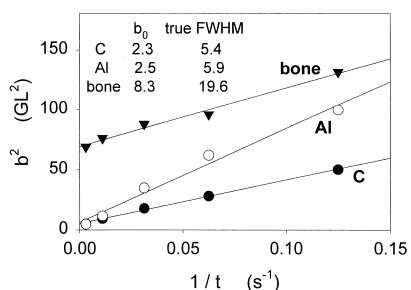


**Figure 2.**  $b^2$ , determined by fitting equation (4) to the gray-level distribution, in dependency of counting time, given in units of  $1/t$ . For C, Al, and bone, four different scanning speeds (8, 16, 100, 330 sec/image) were tested. The other instrument settings were identical to those described in our study.<sup>1</sup> The probe current was set to 0.11 nA and the brightness and contrast were adjusted in such a way that C and Al had gray levels (GL) of 25 and 225, respectively. The values (in units of GL) of the true width,  $b_o$ , and FWHM (full width half maximum) of the distributions were obtained by the intercept of the regression lines with the y axis. (The transformation from  $b_o$  to FWHM is described in the legend to Figure 3.)

To test this theoretical expression (6), we measured gray-level distributions of carbon (C), aluminum (Al), and a bone specimen for a number of counting times, but otherwise identical settings. These distributions were fitted with a gaussian [e.g., equation (4)]. **Figure 2** shows the values of  $b^2$  obtained as a function of  $t$ . The predicted linear dependence [equation (6)] is nicely followed for all the data (linear regression, with  $R^2 > 0.99$ ). The extrapolation to  $1/t = 0$  (limit of extremely long measuring times) yields the true width,  $b_o$ , of the distribution. It is also obvious that the width of the gray-level distributions from C and Al increase dramatically when the counting statistics get worse. The effect for bone is smaller due the much larger inherent width of the distribution. It is also visible that (under the given instrumental conditions), after about 100 sec of counting time, there is no longer a large difference between the measured and the true value. Moreover, the slopes of the curves in Figure 2 give the values for  $K$  and  $M_o$  in equation (6).  $K$  and  $M_o$  are the only two parameters defined by the actual instrument settings (e.g., gain and offset voltage of the BE amplifier) and can be determined for any instrument and instrumental setting, using the procedure just outlined.

To obtain reliable results for the gray-level distribution and, ultimately, for BMDD, it is essential to choose the appropriate counting time for every setting of instrument parameters. **Figure 3** shows the counting time needed to obtain a <5% difference

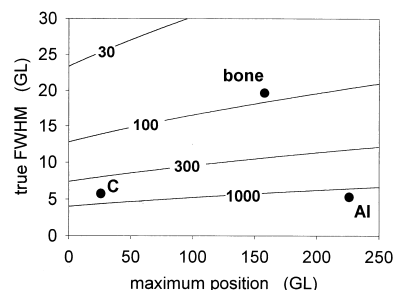


**Figure 3.** Counting time (in sec/image) needed to reach a 5% precision for FWHM is shown for C, Al, and bone (materials different in gray-level distribution maxima), again using standard instrument settings. The true FWHM was calculated by the equation,  $FWHM = b_o(8 \ln 2)^{1/2}$ .

between true and observed distribution width under the instrument settings also used in Figure 2. This estimate is based on equation (6). The main conclusion is that the counting time needed depends on both the true width of the gray-level distribution ( $b_o$ ) and its maximum position ( $M$ ). For bone, a counting time (using the instrument settings given in Figure 2) of about 100 sec appears sufficient, which is precisely the value used in our study.<sup>1</sup>

In conclusion, we have demonstrated that the gray-level histograms of bone shown in our study<sup>1</sup> accurately indicate the mineral content in the samples, thus justifying to scale the distribution in units of percent weight of calcium.

## References

1. Roschger, P., Fratzl, P., Eschberger, J., and Klaushofer, K. Validation of quantitative backscattered electron imaging for the measurement of mineral density distribution in human bone biopsies. *Bone* 23:319–326; 1998.
2. Roschger, P., Fratzl, P., Klaushofer, K., and Rodan, G. Mineralization of cancellous bone after alendronate and sodium fluoride treatment: A quantitative backscattered electron imaging study on minipig ribs. *Bone* 20:393–397; 1997.
3. Roschger, P., Plenck, H., Jr., Klaushofer, K., and Eschberger, J. A new scanning electron microscopy approach to the quantification of bone mineral distribution: Backscattered electron image gray-levels correlated to calcium K $\alpha$ -line intensities. *Scann Microsc* 9:75–88; 1995.

**P. Roschger**  
**P. Fratzl**  
**J. Eschberger**  
**K. Klaushofer**

*Ludwig Boltzmann Institut für Osteologie  
Wien, Austria*